LAWRENCE
LIVERMORE
NATIONAL
LABORATORY

LLNL-PROC-666390

# High-temperature illite dissolution kinetics

M. M. Smith, S. A. Carroll

January 21, 2015

Stanford Geothermal Workshop
Stanford, CA, United States
January 26, 2015 through January 28, 2015

## Disclaimer

PROCEEDINGS, Fortieth Workshop on Geothermal Reservoir Engineering
Stanford University, Stanford, California, January 26-28, 2015
SGP-TR-204

# High-Temperature Illite Dissolution Kinetics

Megan M. Smith and Susan A. Carroll

Atmospheric, Earth, and Energy Division, Lawrence Livermore National Laboratory; 7000 East Avenue; Livermore, CA, USA 94550

megan@llnl.gov; carroll6@llnl.gov

**Keywords:** geothermal geochemistry, illite, dissolution, kinetics

## ABSTRACT

Fluids cycled through producing or engineered geothermal reservoirs are likely to be out of chemical and thermal equilibrium with surrounding rock and mineral phases. Knowledge of the reactivity of common fracture-filling minerals is needed to predict longer-term flow and permeability sustainability in systems where fractures make up a large portion the fluid pathways within the reservoir. Currently the majority of kinetic reaction data for many common fracture-associated phyllosilicate minerals has been obtained at lower temperatures and extrapolation from these data may or may not accurately predict mineral kinetics at geothermal conditions. Here we present rate data and a preliminary kinetic rate formulation for illite (special clay "IMt-1," Clay Minerals Society) dissolution over temperatures of 100-280 °C and pH levels of 3-9. We find that up to temperatures of 280 C, the variation of dissolution rate with pH is surprisingly small (less than 0.5 orders of magnitude)for acid to mildly acidic solutions ($3 < pH < 6$), although rates increase strongly at high (pH ~9) levels. The dependence of the rate itself on temperature also increases in more alkaline solutions. We compare our findings with the data and rate formulation given by Köhler et al. (2003) from experiments performed at lower temperatures (5-50 °C). At temperatures below 200 °C and circumneutral solution pH, Köhler et al.'s (2003) rate formulations fits our new data reasonably well. However, this formulation overpredicts dissolution rates by ~1.5 orders of magnitude at higher pH levels and at temperatures greater than 200 °C. We present an alternative rate formulation_____.

## 1. INTRODUCTION

Development of engineered geothermal syustems (EGS) through the reactivation of fractures in deep hot rocks requires sustained permeability for about 30 years or longer. Chemical reactions pose an important but poorly understood threat to EGS long-term success, because critical kinetic data necessary to fully understand reaction progress are lacking for most fracture-filling minerals at EGS target temperatures (add GRC ref here). The poor understanding of the impact of rock-water interactions on fracture permeability is illustrated by variable results from experimental laboratory studies on fractured rock cores. Some data suggest that chemical reactions can significantly reduce fracture permeability even at temperatures well below EGS target zones (200 to 400 °C; Polak et al., 2003; Carlson et al., 2005; Viani et al., 2005; Yasuhara et al., 2006l, 2011; Yasuhara and Elsworth, 2008), while other experiments in chemically perturbed environments (e.g., undersaturated or $CO_2$-rich fluids) show an increase in fracture permeability (Polak et al., 2004; Smith et al., 2013a). It is important to correctly asses the role of chemistry on EGS permeability, because reductions in fracture permeability will negatively affect heat transfer, possibly rendering the EGS reservoir uneconomic. In principle, the role of geochemistry could be assessed through modeling. Unfortunately, kinetic data and rate equations are lacking for fracture-filling minerals at EGS temperature (200-400 C) and are rare even up to 100 C (Cama et al., 2000; Brandt et al., 2003; Gustaffson and Puigdomenech, 2003; Köhler et al., 2003; Carroll and Knauss, 2005; Lowson et al., 2005, 2007; Smith et al., 2013b). Use of reaction rates extrapolated from low temperature data may overpredict dissolution by up to 10,000 times at typical EGS temperatures, leading to poor estimates of the impact of geochemical alteration in EGS permeability (Smith et al., 2013b).

We partially address this need by measuring dissolution rates and deriving a rate equation for illite, one of several fracture-associated minerals identified in potential shear stimulation zones at several EGS demonstration sites. The resulting rate equation can be directly incorporated into larger-scale reactive transport simulations to assess the impact of geochemical reactions on shear zone permeability. We report new illite dissolution rate measurements obtained over pH levels of 3 to 10, and temperatures from 100 to 280 °C. The resulting rate data and equations are compared with illite dissolution previously measured from 5 to 50 °C (Köhler et al., 2003).

Illite is a 2:1 potassium-bearing aluminosilicate clay mineral, closely related to muscovite but possessing slightly less potassium in its chemical structure. In lower-temperature environments, illite is often found interlayered with smectite, but with increasing temperature the fraction of interlayered smectite generally decreases (e.g., Sass et al., 1987). Illite is extremely abundant in many types of ore deposits and hydrothermal/geothermal systems, as well as in sedimentary sandstone reservoirs, as both a primary or secondary alteration mineral (Sródón and Eberl,1984). The dissolution kinetics of illite are of interest because the abundance of illite has been linked to permeability variations within petroleum reservoirs (Deer et al., 1992) and so may be expected to also play a role in long-term EGS permeability. In addition, only two previous studies have been conducted to examine the kinetics of this mineral, but at temperatures far below typical geothermal conditions (Köhler et al., 2003; Bibi et al., 2011).

## 2. MATERIALS AND METHODS

The illite used in this study was purchased from the Clay Minerals Society as Special Clay IMt-1. The bulk material was mechanically crushed and sieved to collect only the 150-250 um size fraction for use. We note that illite is strictly defined as minerals of ≤ 2 um size; we retained these larger crystal aggregates to ensure that the material would not migrate within the flow-through reactor set-up. In

keeping with previously published geochemical experimental work in similar layered silicates (e.g., Sass et al., 1987; Kohler et al., 2003), this size fraction was further treated with an acid wash to remove potential carbonate impurities (Zavarin et al., 2012). The mineral separates were then dried and re-sieved, and stored for further characterization analysis and kinetic experimentation. The initial surface area of the unreacted solids was measured as 34.2 $g \cdot m^{-2}$ from multi-point $N_2$ BET. The chemical composition was determined by electron microprobe and transmission electron microprobe as $K_{1.55}(Na_{0.04},Ca_{0.04})Al_{2.90}(Fe_{0.70},Mg_{0.54},Ti_{0.05})Si_{6.75}Al_{1.25}O_{20}(OH)_4$. Some remaining trace quantities of quartz and potassium feldspar were detected in both powder diffraction patterns and in the TEM analysis. Comparison of XRD patterns for dry and for ethylene-glycolated samples showed that the sample was predominately illite, with no indication of expandable smectite clays above the resolution of the technique (~5%).

All experiments were performed in a background matrix of reagent-grade 0.05m NaCl and distilled deionized water initially purged with $N_2$ gas to remove atmospheric oxygen. Reagent-grade hydrochloric acid (HCl) and sodium hydroxide (NaOH) were used to adjust the pH of selected individual solutions to desired pH levels. Total chloride levels in the experimental solutions were maintained at a constant value of 0.05m, but sodium levels varied up to 0.075m in some experiments as a result of pH adjustment by sodium hydroxide. Approximately 1g of unreacted illite was used for single temperature/pH flow-through experiments, with larger masses (~1.5g) used in stacked experiments (in which dissolution rates were measured at variable temperature and constant pH using the same solid illite).

Titanium single-pass mixed-flow reactors (e.g., Dove and Crerar, 1990) were used to conduct the illite dissolution experiments over a temperature range of 100-280 °C and a pH range of 3-10 at far-from-equilibrium conditions. A schematic of the experimental set-ups can be found in Smith et al. (2013b). Room-temperature NaCl solutions were pumped into the experimental reactors to pressurize the system, and then the reactor was brought to temperature over a period of several hours while influent solution continued to flow at a constant flowrate of 0.5 $mL \cdot min^{-1}$. Time $t = 0$ in discussion and figures indicates the time when the reactor system achieved its target temperature. Influent solution was pumped past the illite grains, held between fine titanium meshes in an isolated sample holder within the experimental reactor, ensuring continuously mixed conditions. Reactor system pressures were maintained well above boiling point pressures by the use of a dome-loaded back-pressure regulator and nitrogen gas at the reactor outlet. All wetted reactor surfaces including the pump and back-pressure regulator were made of C-276 alloy, passivated grade-4 titanium, or PEEK. To conclude each experiment, the reator heaters were turned off and the sample holder was removed from each reactor as soon as liquid temperatures decreased below 100 C. Sample holders were dried overnight at 60 C and illite solid were then removed and preserved for post0reaction characterization. Reactors were treated between experiments with a mildly acidic (pH 4) HCl solution and 24 hours of distilled water rinsing, and reactor parts were periodically boiled in 8N nitric acid and re-passivated.

Samples were collected directly downstream of the back-pressure regulator through a luer-lock port and were split into three aliquots for analysis: 15 mLs were filtered and acidified for silicon, magnesium, aluminum, iron, and calcium analysis by inductively-coupled plasma optical emission spectrometry (ICP-OES); 1mL was filtered and diluted by 10x with distilled water for ion chromatography (IC) to confirm stable background sodium and chloride concentrations and to analyze for potassium levels; and 3-5 mLs were measured for pH at 20 C. The geochemical code EQ3/6 (Wolery, 1992) and the updated *data0.ymp.R5* database were used to calculate solution pH at experimental temperatures as well as mineral-specific fluid saturation indices.

NOTES ABOUT PEST CODE/USAGE.

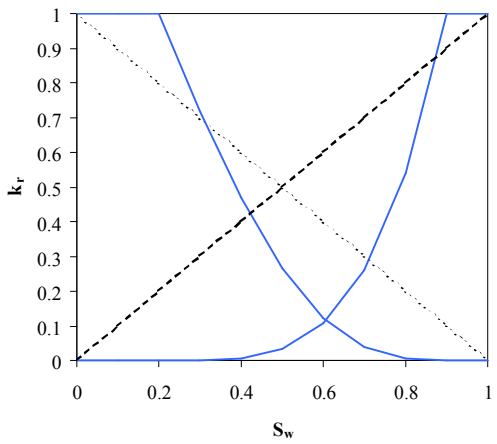


**Figure 1: The figure above is in <Figure Style>. Please paste your figures as "Pictures" (use "Paste Special"). This figure caption is in <FigCaption Style>. Make your figures "in line with text" (not "float over text").**

## 3. RESULTS

Here we present the illite dissolution rate data and derive a rate law from the empirical data collected from pH 3-10 at 100, 150, 200, 250, and 280 °C. We use results from temperature and pH conditions where we have the greatest experimental coverage to describe the effect of solution pH on the rate (with 150 °C data), and temperature dependence of the rate (at acid pH conditions).

### 3.1 Evaluation of the Experimental Data

The net illite dissolution rates were determined from a steady-state change in measured effluent composition, normalized to flowrate, total surface area, and stoichiometric coefficient, as described by equation (1):

$$R_{net} = \frac{C_i \cdot \nu}{m_{illite} \cdot A_{illite} \cdot \sigma_i} \quad (1)$$

The net rates, $R_{net}$ (mole·m$^{-2}$·s$^{-1}$), were calculated from steady-state levels of dissolved Si (here, *i*) in effluent samples, $C$ (mol·L$^{-1}$); the initial mass of illite present in each experiment, $m_{illite}$ (g); the measured illite surface area, $A_{illite}$ (m$^2$·g$^{-1}$); the stoichiometry of Si present in the illite mineral formula, σ; and the constant flowrate, υ (L·s$^{-1}$). The net dissolution rates, steady-state solution composition, and saturation indices for each experiment are listed in Table 1. An example dataset of trends in solution composition is shown in Figure 1 for an experiment conducted at a temperature of 100 °C and influent pH = 7.4. Steady-state was defined as the time period in which concentrations of primary illite-forming elements (Si, ±Al, ±K) varied by less than 10%, represented in Figure 1 by the last three data points collected between 140 and 250 hours for this experiment.

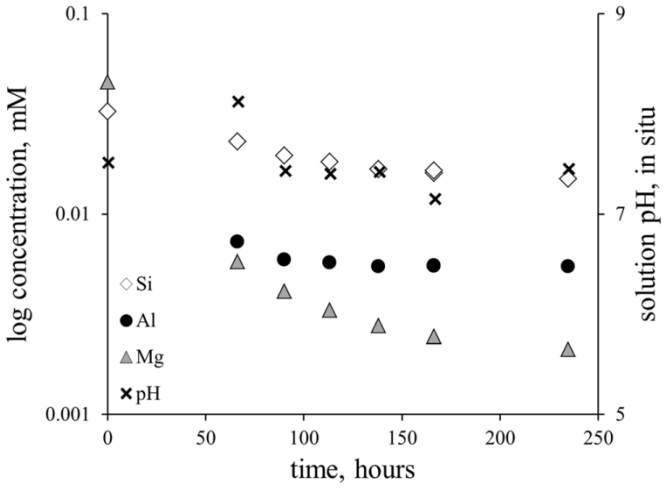


**Figure 2: Typical experimental solution chemistry as a function of time for illite dissolution experiments conducted at neutral and basic pH solutions (here, dissolution at 100 °C, influent pH = 7.4).**

Dissolution rates of alumino-silicate minerals like illite typically exhibit a parabolic dependence on pH, such that faster rates at acid or alkaline pH conditions decrease to minimum values in more neutral solutions, similar to the trend seen in the 5-50 °C data collected by Köhler et al. (2003). However, our results from 100 to 280 °C suggest a different dependence on pH, which is best illustrated by the data collected at 150 °C across a wide pH range (Figure 2). The results show that illite dissolution is largely constant from pH 2 – 6, with increases in the rate occurring only for pH > 6. This trend is also apparent at 100, 200, 250, and 280 °C, with additional experiments in progress to confirm this relationship between rate and pH. The difference between the pH dependences observed at 50 °C and these seen at 150 °C and acid pH conditions may reflect secondary mineral precipitation, a less dominant acid-catalyzed dissolution mechanism at higher temperatures, or an effect of reaction affinity.

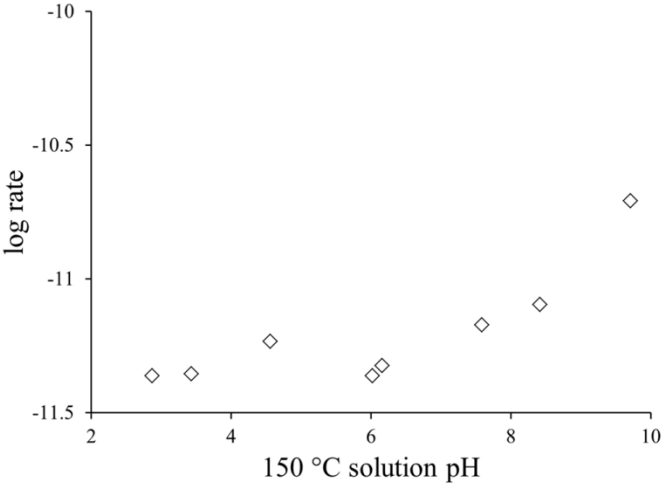


**Figure 2: Illite dissolution rate (derived from steady-state [Si] concentrations) versus pH, from 150 °C experiments.**

Comparison of dissolution rates calculated with dissolved aluminum and silica suggest that aluminum hydroxides may have precipitated from the solution. Figure 3 plots the ratio of dissolution rates estimated from steady-state aluminum and silica concentrations for all experiments from this study. Aluminum is depleted below the detection limit from pH 2 – 5 and progressively approaches stoichiometric dissolution levels (Al/Si ≈ 0.6) over pH 5 – 10. The non-stoichiometric dissolution noted at more acidic pH is strong evidence for the precipitation of an aluminum-bearing phase, and precipitation of aluminum solids is consistent with retrograde solubility of aluminum at higher temperature and has been observed for feldspars at temperature up to 130 °C (Bourcier et al., 1990; Carroll and Knauss, 2005).

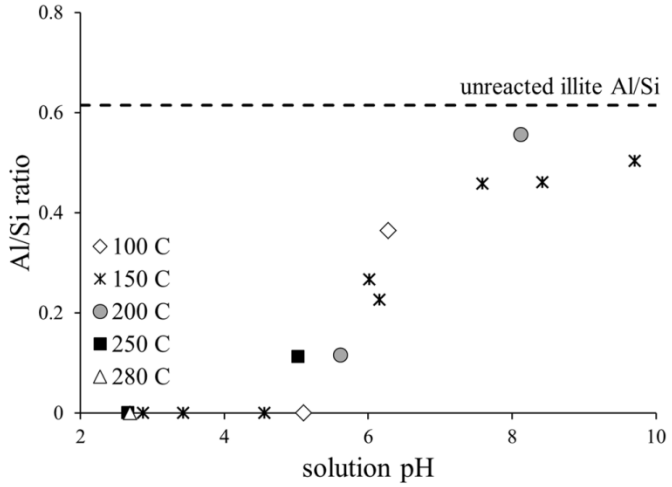


**Figure 3: Ratio of steady-state Al/Si concentrations, mass basis, as a function of pH. Different experimental temperatures are indicated by different symbols. Data plotting on the abscissa are ratios estimated using the Al detection limit as a proxy for [Al] concentrations. The ratio of Al/Si in the unreacted illite solid material is shown by the dashed horizontal line.**

Possible precipitation of aluminum-bearing solids is further supported by saturation index results for several key mineral phases. The saturation index of a fluid with respect to a mineral phase is defined as:

$$SI = \log \frac{Q}{K_{eq}} \tag{2}$$

where $Q$ is the ion activity product and $K_{eq}$ is the equilibrium constant or solubility of the mineral phase. Positive SI values indicate supersaturation of the fluid/potential for mineral precipitation, and negative values indicate fluid undersatuation/potential for mineral dissolution. Figure 4 plots the steady-state saturation indices for the 150 °C experiments versus pH. In this analysis we used the aluminum detection limit (0.05 ppm) as a proxy maximum for those samples where aluminum levels were below detection limits. The solutions are very close to equilibrium with gibbsite, $Al(OH)_3$, at pH 3-7.8, and to kaolinite, $Al_2Si_2O_5(OH)_4$, equilibrium over pH 3-6. In principle, solutions near equilibrium indicate that gibbsite and kaolinite *could* precipitate. If kaolinite precipitation were to fully explain the constant rate values measured over pH 2-6, we would expect to see increasingly supersaturated or at least consistently saturated fluids with respect to kaolinite at decreased/more acidic pH levels. However, this does not appear to be the case, because solutions become more undersaturated (note that SI values represent logarithmic changes in fluid/mineral saturation conditions) at increasingly acidic pH levels. Re-analysis of the solutions with more sensitive methods to more accurately determine aluminum concentrations and kaolinite saturation indices, as well as analysis of reacted solids for evidence of precipitated secondary minerals with X-ray diffraction and/or high-resolution TEM, should resolve this issue. If evidence of secondary precipitates is noted, the rates could be theoretically corrected for aluminosilicate precipitation through comparison of stoichiometric release of K relative to Si. For the remainder of this paper we will assume that the measured dissolution rates are not affected by potential kaolinite precipitation.

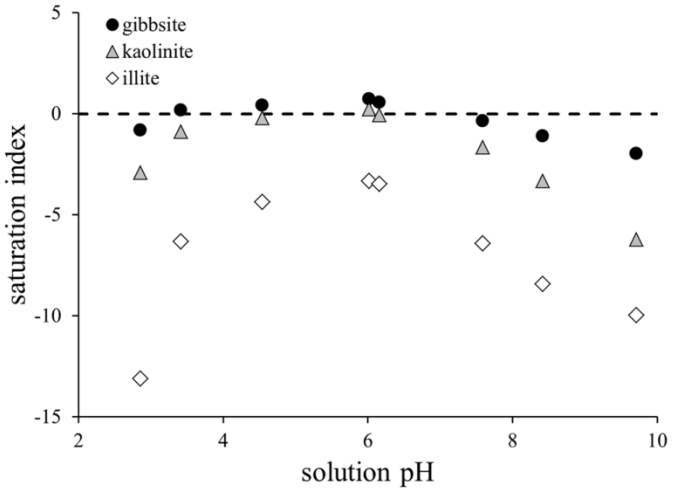


**Figure 4: Saturation indices (log IAP/$K_{eq}$) versus in situ solution pH, for all experiments conducted at 150 °C. Saturation indices for experiments at pH 2-5 were estimated using the Al detection limit.**

Constant rates in acid pH regions may alternatively be attributed to a slowing down of the rate due to the solutions' approach to equilibrium. In many reactive-transport simulators, this behavior is typically captured using a rate form which includes a reaction affinity term. The generic rate equation, derived from transition state theory (Lasaga, 1995), consists of acid, neutral, and alkaline dissolution terms related to solution temperature, pH, and composition as:

$$R_{net} = f(\Delta G_r)\cdot\left[\left(k_{acid,298K}\cdot e^{\frac{-E_{acid}}{R}\cdot\left(\frac{1}{T}-\frac{1}{298}\right)}\cdot a_{H+}^{n}\right)+\left(k_{neut,298K}\cdot e^{\frac{-E_{neut}}{R}\cdot\left(\frac{1}{T}-\frac{1}{298}\right)}\right)+\left(k_{basic,298K}\cdot e^{\frac{-E_{basic}}{R}\cdot\left(\frac{1}{T}-\frac{1}{298}\right)}\cdot a_{OH-}^{m}\right)\right] \quad (2)$$

where $k$ represents reaction rate constants at 25 °C for specific rate mechanisms (acid, neutral, or alkaline), $E$ represents activation energy values, $a_i$ is the activity of species $H^+$ or $OH^-$ for which $n$ and $m$ are the respective reaction order for the $H^+$ or $OH^-$-promoted rates, R represents the gas constant, and $f(\Delta G_r)$ is an expression relating the rate to the dissolution reaction affinity, or approach of the fluid system towards equilibrium with the dissolving mineral. If reaction affinity were to play a key role in the net dissolution rate at acid pH, then the saturation index of steady-state solutions should approach illite equilibrium with increasingly acidic pH. However, the reverse is observed in Figure 4: solutions become increasing undersaturated with respect to illite from as pH decreases from 6 to 2. Progressively more undersaturated solutions at acidic pH support the notion that the rates are independent of $\Delta G_r$.

### 3.2 Derivation of Kinetic Rate Equation

We assume here that the non-stoichiometric dissolution represents the precipitation of only an aluminum-bearing phase (e.g., gibbsite) and that illite dissolution rates can be derived from dissolved silica concentrations. This is a fairly significant assumption which must be justified through analysis of reacted solids for secondary phases using high-resolution TEM and by detailed analysis of dissolved potassium concentrations. Illite dissolution rate data collected in these experiments from 100 to 280 °C is best modeled with a revised form of equation (2) consisting of terms that account for constant rates from pH 2 to 6 and increasing rates at pH > 6.

$$q = \frac{k}{\mu}\,\mathrm{A}\,\left(\frac{\Delta p}{L}\right) \quad (3)$$

We adopt the "neutral" and "basic" nomenclature for the dissolution mechanisms to be consistent with literature, even though the "neutral" mechanism extends into acid pH levels at elevated temperatures. Because $k$ and $E$ values for one mechanism are strongly correlated, an apparent activation energy value for each mechanism is extracted from plots of the rates versus $T^{-1}$, for experiments conducted at pH < 5, and at pH ≈ 8, to capture the temperature dependence in each region (Figure 5). In both figures the slope of the best-fit line through the data is proportional to the activation energy divided by the gas constant, with $E_{neut}$ = 14.0 kJ·mole$^{-1}$ and $E_{basic}$ = 43.7 kJ·mole$^{-1}$. The reaction order for the basic mechanism, $m$ = 0.30, is estimated from the pH dependence of 150 °C rate data over a pH range of 6-10. Rate constants at the reference temperature of 100 C are extrapolated from Figure 5

## 4. CONCLUSIONS

The objective of this suite of experiments was to develop a useful kinetic expression for illite dissolution that is applicable over a wide range of solution pH and temperature conditions representation of subsurface conditions in natural and/or engineered geothermal reservoirs. The resulting rate equation is dependent on both pH and temperature and utilizes two specific dissolution mechanisms (a "neutral" and a "basic" mechanism). The form of this rate equation should be amenable to inclusion in most existing reactive transport codes for use in prediction of rock-water interaction and consequences in geothermal systems.

Existing low-temperature rate equations should not be used to forecast the impacts of illite dissolution in high-temperature EGS applications, because the acid-promoted mechanism no longer appears to contribute to dissolution at temperatures above 100 °C. At this time, we recommend that models use rate equations that are specific to the temperature range of their study. The three-part acid/neutral/basic rate equation of Kohler et al. (2003) should be used for systems below 50 °C, and the two-part neutral/basic rate equation:

should be used above 100 C.

**ACKNOWLEDGEMENTS**

We acknowledge support of this research through the U.S. Department of Energy, Geothermal Technologies Program. We also wish to thank Cora Madden (LLNL) for ICP-OES solution analysis. This work performed under the auspices of the U.S> Department of Energy by Lawrence Livermore National Laboratory under Contract DE-AC52-07NA27344. LLNL-CONF-XXXXXX.

**REFERENCES**

Bibi, I., Singh, B., and Silvester, E.: Dissolution of illite in saline-acidic solutions at 25 °C, *Geochimica et Cosmochimica Acta*, **75**, (2011), 3237-3249.

Bourcier, W.L., Knauss, K.G., Jackson, K.J.: Aluminum hydrolysis constants to 250 °C from boehmite solubility measurements, *Geochimica et Cosmochimica Acta*, **57**, (1993), 747–762.

Brandt F., Bosbach, D., Krawczyk-Bärsch, R., Arnold, T., and Bernhard, G.: Chlorite dissolution in the acid pH range: A combined microscopic and macroscopic approach, *Geochimica et Cosmochimica Acta*, **67**, (2005), 1451-1461. 10.1016/S0016-7037(02)01293-O.

Cama, J., Ganor, J., Ayora, C., and Lasaga, C.A.: Smectite dissolution kinetics at 80°C and pH 8.8, *Geochimica et Cosmochimica Acta*, **64**, (2000), 2701-2717.

Carlson, S.R., Roberts, J.J., Detwiler, R.L., Viani, B.E., and Roberts, S.K.: Fracture permeability evolution in Desert Peak quartz monzonite, *GRC Transactions*, **29**, (2005), 337-342.

Carroll, S.A., and Knauss, K.G.: Dependence of labradorite dissolution kinetics on $CO_{2(aq)}$, $Al_{(aq)}$, and temperature, *Chemical Geology*, **217**, (2005), 213-225.

Deer, W.A., Howie, R.A., and Zussman, J. (1992) An introduction to the rock-forming minerals, 2nd ed. Addison Wesley Longman Limited, Essex, England, 696pp.

Dove, P.M., and Crerar, D.A.: Kinetics of quartz dissolution in electrolyte solutions using a hydrothermal mixed flow reactor, *Geochimica et Cosmochimica Acta*, **54**, (1990), 955-969. 10.1016/0016-7037(90)90431-J.

Gustaffson A.B., and Puigdomenech, I.: The effect of pH on chlorite dissolution rates at 25 °C, *Materials Research Society Symposium Proceedings*, **757**, (2003), 649-655. 10.1557/PROC-757-II3.16

Köhler, S.J., Dufaud, F., and Oelkers, E.H.: An experimental study of illite dissolution kinetics as a function of pH from 1.4 to 12.4 and temperature from 5 to 50°C, *Geochimica et Cosmochimica Acta*, **67**, (2003), 3583-3594.

Lasaga, A.C. (1995) Fundamental approaches to describing mineral dissolution and precipitation rates. In *Reviews in Mineralogy, Volume 31: Chemical Weathering Rates of Silicate Minerals* (eds. A.F. White and S.L. Brantley). Mineralogical Society of America, Washington, D.C., pp.23-86.

Lowson R.T., Comarmond, M-C.J., Rajaratnam, G., and Brown, P.L.: The kinetics of the dissolution of chlorite as a function of pH and at 25°C, *Geochimica et Cosmochimica Acta*, **69**, (2005), 1687-1699. 10.1016/j.gca.2004.09.028.

Lowson R.T., Brown, P.L., Comarmond, M-C.J., and Rajaratnam, G.: The kinetics of chlorite dissolution, *Geochimica et Cosmochimica Acta*, **71**, (2007), 1431-1447. 10.1016/j.gca.2006.12.008.

Polak, A., Elsworth, D., Yasuhara, H., Grader, A.S., and Halleck P.M.: Permeability reduction of a natural fracture under net dissolution by hydrothermal fluids, *Geophysical Research Letters*, **30**, (2003), 2020. 10.1029/2003GL017575.

Sass, B.M., Rosenberg, P.E., and Kittrick, J.A.: The stability of illite/smectite during diagenesis: An experimental study, *Geochimica et Cosmochimica Acta*, **51**, (1987), 2103-2115.

Smith, M.M., Walsh, S.D.C., McNab, W.W., and Carroll, S.A.: Experimental investigation of brine-$CO_2$ flow through a natural fracture: Permeability increases with concurrent dissolution/reprecipitation reactions, *Proceedings*, 38th Workshop on Geothermal Reservoir Engineering, Stanford University, Stanford, CA (2013a).

Smith, M.M., Wolery, T.J., and Carroll, S.A.: Kinetics of chlorite dissolution at elevated temperatures and $CO_2$ conditions, C*hemical Geology*, **347**, (2013b), 1-8. 10.1016/jchemgeo.2013.02.017.

Sródón, J., and Eberl, D.D. (1984) Illite. In *Reviews in Mineralogy, Volume 13: Micas* (ed. S.W. Bailey). Mineralogical Society of America, Washington, D.C., pp.495-544.

Viani, B.E., Roberts, J.J., Detwiler, R.L., Roberts, S.K., and Carlson, S.R.: Simulating injectate/rock chemical interaction in fractured Desert Peak quartz monzonite, *GRC Transactions*, **29**, (2005), 425-430.

Yasuhara, H., Polak, A., Mitani, Y., Grader, A.S., Halleck, P.M., and Elsworth, D.: Evolution of fracture permeability through fluid-rock reaction under hydrothermal conditions, *Earth and Planetary Science Letters*, **244**, (2006), 186-2000.

Yasuhara, H., Kinoshita, N., Ohfuji, H., Lee, D.S., Nakashima, S., and Kishida, K.: (2011) Temporal alteration of fracture permeability in granite under hydrothermal conditions and its interpretation by coupled chemo-mechanical model, *Applied Geochemistry*, **26**, (2011), 2074-2088.

Zavarin, M., Powell, B.A., Bourbinm M., Zhao, P., and Kersting, A.B.: Np(V) and Pu(V) ion exchange and surface-mediated reduction mechanisms on montmorillonite, *Environmental Science and Technology*, **46**, (2012), 2692-2698.